

A New Subtype of Brachydactyly Type B Caused by Point Mutations in the Bone Morphogenetic Protein Antagonist NOGGIN

K. Lehmann,* P. Seemann,* F. Silan, T. O. Goecke, S. Irgang, K. W. Kjaer, S. Kjaergaard, M. J. Mahoney, S. Morlot, C. Reissner, B. Kerr, A. O. M. Wilkie, and S. Mundlos

Brachydactyly type B (BDB) is characterized by terminal deficiency of fingers and toes, which is caused by heterozygous truncating mutations in the receptor tyrosine kinase-like orphan receptor 2 (*ROR2*) in the majority of patients. In a subset of *ROR2*-negative patients with BDB, clinically defined by the additional occurrence of proximal symphalangism and carpal synostosis, we identified six different point mutations (P35A, P35S, A36P, E48K, R167G, and P187S) in the bone morphogenetic protein (BMP) antagonist NOGGIN (*NOG*). In contrast to previously described loss-of-function mutations in *NOG*, which are known to cause a range of conditions associated with abnormal joint formation but without BDB, the newly identified BDB mutations do not indicate a major loss of function, as suggested by calculation of free-binding energy of the modeled *NOG*-*GDF5* complex and functional analysis of the micromass culture system. Rather, they presumably alter *NOG*'s ability to bind to BMPs and growth-differentiation factors (GDFs) in a subtle way, thus disturbing the intricate balance of BMP signaling. The combined features observed in this phenotypic subtype of BDB argue for a functional connection between BMP and *ROR2* signaling and support previous findings of a modulating effect of *ROR2* on the BMP-receptor pathway through the formation of a heteromeric complex of the receptors at the cell surface.

Brachydactyly is shortness of the fingers and/or toes (digits), usually inherited as a dominant trait. It most often occurs as an isolated physical feature but can also be part of a more complex set of anomalies such as a skeletal dysplasia or a congenital malformation syndrome. According to their pattern of skeletal hand malformation, the different isolated brachydactylies have been classified into the subtypes A–E.¹ Brachydactyly type B (BDB), the most severe form, is characterized by aplasia or hypoplasia of the distal and middle phalanges of digits II–V. In less severe cases, hypoplasia of the distal phalanx is associated with hypoplasia of the nails and fusion of distal interphalangeal joints. To date, heterozygous mutations in the gene encoding the receptor tyrosine kinase-like orphan receptor 2 (*ROR2* [GenBank accession number NM_004560]) have been reported to be the cause of BDB1 (MIM 113000) in the majority of affected individuals. These mutations cluster in two regions, resulting in truncation of the receptor of either the N-terminal or C-terminal of the intracellular tyrosine kinase domain.^{2,3}

The patients described here were screened for mutations

in *ROR2*, but no mutations were identified. *ROR2*-negative BDB has been described before, indicating genetic heterogeneity of the disorder, but the molecular basis in this group of patients was not known. Previous studies have shown that *BMPRI1B*, the high-affinity receptor for *GDF5*, interacts with *ROR2*.⁴ We therefore sequenced *GDF5*, *BMPRI1B*, and the inhibitor of *GDF5*—*NOGGIN* (*NOG* [GenBank accession number NM_005450])—in all *ROR2*-negative subjects. Informed consent for genetic analyses was obtained from all patients or their legal guardians. Molecular testing was performed on purified genomic DNA obtained from venous blood samples. The primer sequences and PCR conditions for the molecular testing can be found elsewhere (for *ROR2*,³ for *GDF5*,⁵ and for *BMPRI1B*⁶). The *NOG*-coding region was amplified in two overlapping segments, with use of the following primer pairs: 1-1 forward (5'-CTCGGCGTGCTCTCCTC-3') and 1-1 reverse (5'-GCTTAGGCGCTGCTTCTTG-3'), which produced a PCR product of 476 bp, and 1-2 forward (5'-ACCTGGCGGAGCTGGAC-3') and 1-2 reverse (5'-GAACTGGTTGGAGGCGG-3'), which produced a PCR product of 479

From the Institut für Medizinische Genetik, Universitätsmedizin Berlin Charité (K.L.; S. Mundlos), and Max-Planck-Institut für Molekulare Genetik (P.S.; S.I.; S. Mundlos), Berlin; Department of Medical Genetics, Duzce School of Medicine, Duzce University, Duzce, Turkey (F.S.); Institut für Humangenetik und Anthropologie, Heinrich-Heine-Universität, Düsseldorf (T.O.G.); Wilhelm Johannsen Centre for Functional Genome Research, Institute of Cellular and Molecular Medicine, University of Copenhagen, Copenhagen (K.W.K.); Department of Medical Genetics, John F. Kennedy Institute, Glostrup, Denmark (S.K.); Department of Genetics, Yale University School of Medicine, New Haven, CT (M.J.M.); Praxis für Humangenetik, Ärztliche Partnerschaft Wagner-Stibbe Hannover, Hannover (S. Morlot); Institut für Biologie, Molekulare Neurobiologie, Otto-von-Guericke-Universität, Magdeburg, Germany (C.R.); Regional Genetic Service, Royal Manchester Children's Hospital, Manchester United Kingdom (B.K.); and Weatherall Institute of Molecular Medicine, John Radcliffe Hospital, University of Oxford, Oxford, United Kingdom (A.O.M.W.)

Received March 15, 2007; accepted for publication April 26, 2007; electronically published June 8, 2007.

Address for correspondence and reprints: Dr. K. Lehmann, Institut für Medizinische Genetik, Universitätsmedizin Berlin Charité, Augustenburger Platz 1, 13353 Berlin, Germany. E-mail: katarina.lehmann@charite.de

* These two authors contributed equally to this work.

Am. J. Hum. Genet. 2007;81:388–396. © 2007 by The American Society of Human Genetics. All rights reserved. 0002-9297/2007/8102-0019\$15.00
DOI: 10.1086/519697

bp. PCR conditions can be obtained on request. Sequencing was done using the ABI Prism BigDye Terminator Sequencing Kit (Applied Biosystems), with PCR primers used as sequencing primers. Products were evaluated on an automated capillary sequencer (Applied Biosystems).

We discovered heterozygosity for five different missense mutations in *NOG* in six familial cases (c.103C→G [P35A], c.103C→T [P35S], c.106G→C [A36P], c.142G→A [E48K], and c.559 C→T [P187S]), originating from Germany, Turkey, Denmark, Iran, and the United Kingdom. In one patient from North America, a de novo mutation, c.499C→G (R167G), confirmed by molecular testing in the unaffected parents, was detected. Heterozygous mutations in *NOG* have been reported elsewhere to be associated with several human disorders characterized by abnormal joints, including proximal symphalangism (SYM1 [MIM 185800]), tarsal-carpal coalition syndrome (TCC [MIM 186570]), multiple synostosis syndrome (SYNS1 [MIM 186500]), and stapes ankylosis with broad thumb and toes without symphalangism (MIM 184460).⁷⁻¹⁰

In five of the six families, DNA samples from additional family members were available for *NOG* screening. Sequence analysis demonstrated that the *NOG* mutations segregated with the phenotype with an autosomal dominant inheritance in a total of 24 meioses (fig. 1). All patients exhibited a distinct clinical phenotype, featuring absent/hypoplastic terminal and/or middle phalanges with an amputation-like phenotype similar to that observed in BDB (fig. 2A). In most patients, fingers IV and V showed a severe transverse distal reduction, and fingers II and III were less severely affected. In those fingers in which the distal phalanges were present, abnormal proximal interphalangeal joints were observed, which resulted in the inability to bend the fingers and in missing flexion creases. The most severely affected patients showed a BDB phe-

notype, with an entire aplasia of the distal and middle phalanges of digits II–V. A few of the patients had a milder phenotype, featuring hypoplastic distal phalanges II–V. We categorized the phenotypic expression observed in the patients' hands into three groups: mild (distal phalanges of fingers II–V present but hypoplastic); intermediate (absent distal and sometimes middle phalanges of ulnar rays [fingers IV and V more severely affected than fingers II and III]), and severe (distal and sometimes middle phalanges of fingers II–V absent) (table 1).

In those individuals in whom fingers II–V consisted of two or three phalanges, a fusion of the proximal interphalangeal joints (SYM1) was typically present. Fusion of the distal interphalangeal joints (distal symphalangism [SYM]), similar to fingers observed in patients with *ROR2* mutations associated with a mild phenotype, was additionally observed in patients showing a mild BDB who carried an E48K or a P187S *NOG* mutation. The available radiographs of the adult patients' hands and feet verified the phalangeal joint fusions. In addition, they revealed a coalition of carpal and tarsal bones leading in the hands to a small metacarpus with abnormally configured bones. In two children, we observed an acceleration of bone age. In a newborn girl, an accelerated development of carpal bones of ~6 mo was present (radiographs not shown). In a 6-mo-old child, the status of carpal bones corresponded to the development of a 3-year-old child (fig. 2B [magnification in fig. 2c]). In the latter case, the distance between the hamate and the triquetral bones was narrowed, indicating a future fusion of those two bones, and the proximal epiphysis of metacarpal bone I was unusually formed, caused by an accelerated ossification. The thumbs were proximally set in the majority of patients, because of short first metacarpal bones. Cutaneous syndactyly, particularly between fingers II and III and between fingers III

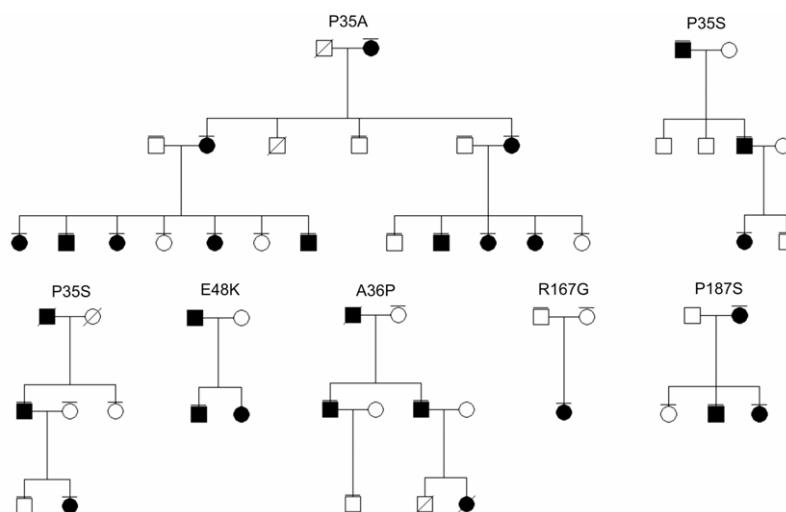


Figure 1. Pedigrees of families with identified *NOG* mutations, as indicated. Affected persons are indicated by blackened symbols. Symbols with horizontal lines indicate individuals for whom mutation analysis was performed.

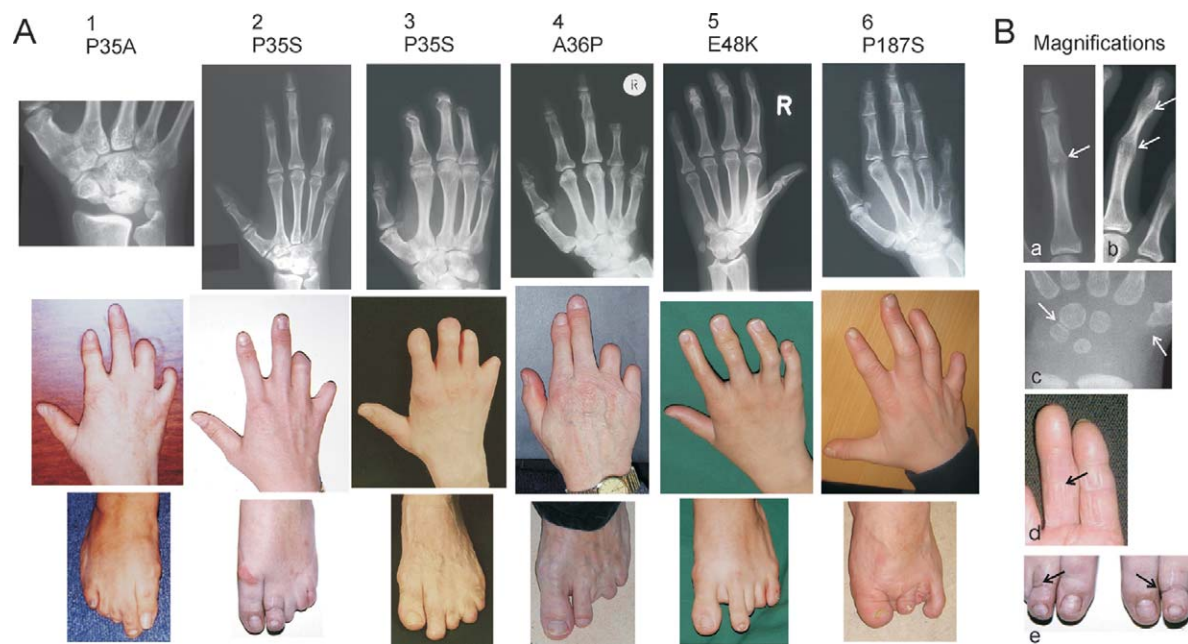


Figure 2. Clinical phenotypes caused by the *NOG* mutations. In panel A, pictures in each vertical group belong to one patient; corresponding mutations are depicted above. In hands, note variable terminal deficiency of fingers. Terminal deficiency—particularly of phalanges IV and V, with a milder involvement of distal phalanges II and III (“intermediate” BDB in table 1)—are depicted in patients 1, 2, 4, and 6. Severely affected hands with absent distal and middle phalanges of fingers II–V (“severe” BDB in table 1) are shown in patient 3. Hypoplastic but present distal phalanges of fingers (“mild” BDB in table 1) are shown in patient 5. Note proximally set thumbs and additional cutaneous syndactyly in some affected hands. Radiographs show proximal SYM of fingers II–V, present in fingers consisting of at least two phalanges. Fusion of carpal bones is a further typical feature (in patient 1, note the atypically configured carpal bones with fusion of hamate, capitate, trapezoid, and trapezium). Shortened metacarpal bones I can be seen in most affected hands. In feet, toes are similarly affected (patient 6 had surgical removal of toes). *B*, Magnifications. *a*, Proximal SYM. *b*, Proximal and distal SYM, as observed in patient 5. *c*, Accelerated development of carpal bones and the proximal epiphysis of metacarpal bone I in a 6-mo-old child. Note narrowed distance between hamate and triquetrum, indicating a future fusion. *d*, Absent flexion creases due to the fused interphalangeal joints. *e*, Symmetric constriction rings in the middle of both second toes in patient 2, imitating a condition caused by amniotic bands.

and IV, was observed as an associated feature. The patients’ feet were affected in a similar way. Toes II–V showed terminal deficiency to a variable degree, and they were stiffened if they consisted of more than one phalanx. The big toes appeared normal. Interestingly, we observed symmetric constrictions in the middle of both second toes in one of the described patients (fig. 2*B* [magnification in fig. 2*e*]). This phenotype imitates a condition typically caused by amniotic bands. Sensorineural hearing loss and farsightedness were observed in a few patients. The overall clinical manifestations of the investigated patients are summarized in table 1.

Our clinical data describe a new subtype of brachydactyly characterized by hypoplasia/aplasia of distal phalanges in combination with (1) SYM, (2) fusion of carpal/tarsal bones, and (3) partial cutaneous syndactyly. We propose to call this type of hand/foot malformation “brachydactyly type B2” (BDB2), because of its striking similarity to BDB1. A clinical description of a family published by Herrmann¹¹ and some of the patients reported by Maro-

teaux et al.¹² seem to have a comparable phenotype, with variable brachydactyly and associated joint fusions.

We excluded a *NOG* mutation in BDB-affected family 3 described by Oldridge et al.¹³ in 1999; the family was also negative for mutations in *ROR2*, indicating that at least one further locus for BDB exists.

In the patients presented here, the P35S mutation in *NOG* was identified in two unrelated individuals, whereas each of the changes P35A, A36P, E48K, R167G, and P187S was detected once. The mutation R167G occurred de novo. All detected changes cosegregate with the BDB2 phenotype, affect highly conserved amino acids of *NOG* (data not shown), are not present in 200 control individuals, and are thus likely to represent pathogenic mutations.

Overall, we identified six different *NOG* mutations. The mutations altering codons 36, 167, and 187 are novel, whereas *NOG* mutations affecting codons 35 and 48 have been described elsewhere in association with abnormal joint fusions in hands and feet.^{7,8,14} In a woman carrying the same E48K mutation, an association of premature

Table 1. Summary of the Clinical Data Correlated with the Identified *NOG* Mutations

Mutation	Incidence of Phenotype						
	BDB			Distal SYM	Carpal Coalition	Shortened MC I ^d	Cutaneous Syndactyly
	Mild ^a	Intermediate ^b	Severe ^c				
P35A	2/12	10/12			8/8	8/8	8/8
P35S		3/6	3/6		5/5 ^e	5/5	4/6
A36P		4/4			2/2	0/2	0/4
E48K	2/4	2/4		+	2/2	2/2	0/4
R167G			2/2		1/2 ^f	0/2	0/2
P187S	3/6	3/6		+	2/2	1/2 ^g	6/6

NOTE.—All subjects had proximal SYM. Each hand of the patients was counted separately. Radiographs were not available for all affected individuals. For each of the listed features, the observed phenotypes refer to the total number of available data (as indicated after the slash).

^a Distal phalanges and nails present, but hypoplastic in fingers II–V.

^b Absent distal and sometimes middle phalanges of fingers IV and/or V (more affected by BDB than are fingers II and III).

^c Absent distal (and middle) phalanges of fingers II–V.

^d MC I = metacarpal bone I.

^e Two of five are x-rays of a 6-mo-old child; both hands showed an accelerated carpal bone age of ~2.5 years.

^f In x-rays of a newborn, both hands showed an accelerated carpal bone age of ~6 mo.

^g Additionally shortened MC IV and V.

ovarian failure, proximal and distal SYM, TCC, and shortness of single fingers and toes with hypoplastic fingernails was reported.¹⁴ The P35S change is listed as a SNP, but screening of 200 control individuals did not show any alteration at codon 35 in *NOG*. Furthermore, the P35S mutation was identified in an Italian family with SYM1.¹⁵ In the clinical description of an affected father and son, additional hypoplasia of distal phalanges was mentioned. Another mutation at position 35, a change from proline to arginine (P35R), described twice elsewhere, resulted either in isolated SYM1 or in TCC.^{7,8} These data support an essential function of the amino acid P35 in *NOG*.

NOG is an extracellular antagonist of bone morphogenetic proteins (BMPs) and growth-differentiation factors (GDFs). The BMP family of secreted molecules has multiple roles in early embryonal development and particularly in skeletogenesis. BMPs and GDFs promote the proliferation and differentiation of mesenchymal precursor cells into chondrocytes and/or osteoblasts and initiate and control the formation of joints at specific regions.¹⁶ GDF5 plays an essential role in chondrocyte differentiation and in the fine tuning of phalangeal development.^{17,18} This complex regulation of BMP and GDF activity is specifically modulated by inhibition through the presence of several BMP antagonists, like *NOG*.^{19,20}

The proteins of the BMP family exert their effect via two different types of BMP receptors: the type I (BMPRI1B and BMPRI1A) and the type II receptors. The affinities of ligands toward the BMP receptors differ. For example, GDF5 binds with a high affinity to BMPRI1B, whereas BMP2 can bind to both BMPRI1A and BMPRI1B. After ligand binding, the BMP type I receptors get activated through the BMP type II receptor by a phosphorylation process leading to intracellular downstream signaling of SMAD (homolog of

mothers against decapentaplegic, *Drosophila*) proteins and the MAP (mitogen-activated protein) kinase pathway.^{21,22} *NOG* binds to BMPs and thereby masks the BMP type I and II receptor-binding sites of certain BMPs and GDF5,^{23,24} and, subsequently, no signaling is initiated.^{25–27}

To elucidate the possible molecular mechanisms by which these newly identified mutations in *NOG* may act to produce BDB in combination with joint fusions, we superimposed the altered amino acid residues on the known three-dimensional structure of human *NOG* (fig. 3). The structure of the complex has been modeled by alignment of the sequence of human GDF5 on the Protein Data Bank (PDB) coordinates of the BMP7 dimer within the *NOG*:BMP7 structure (PDB entry 1M4U), which was solved by x-ray crystallography.^{24,28} The type I and II receptor-binding sites have been determined using PP_SITE.²⁹ The estimated reduction of free-binding energy was calculated for each *NOG* mutant by FOLD-X.^{29,30} The free-binding energy of the complex formation of wild-type (WT) *NOG* and GDF5 was calculated and set to 100% (table 2). The comparison of the free-binding energy of WT *NOG* versus the *NOG* mutants to GDF5 shows that the mutation P35R, which is known to be associated with SYM1 or TCC (but not BDB), has the highest loss of free-binding energy (51%). The BDB2-associated mutations showed a less severe reduction in free-binding energy. The mutations P35A resulted in 14% and P35S in 31% relative loss of free-binding energy; the mutation P187S resulted in 16% loss of free-binding energy. The remainder of BDB2-related mutations at positions A36, E48, and R167 led to reductions of <6%. Thus, the behavior of the majority of BDB2 mutations is similar to that of WT *NOG*, and BDB2 mutations are able to antagonize GDF5 func-

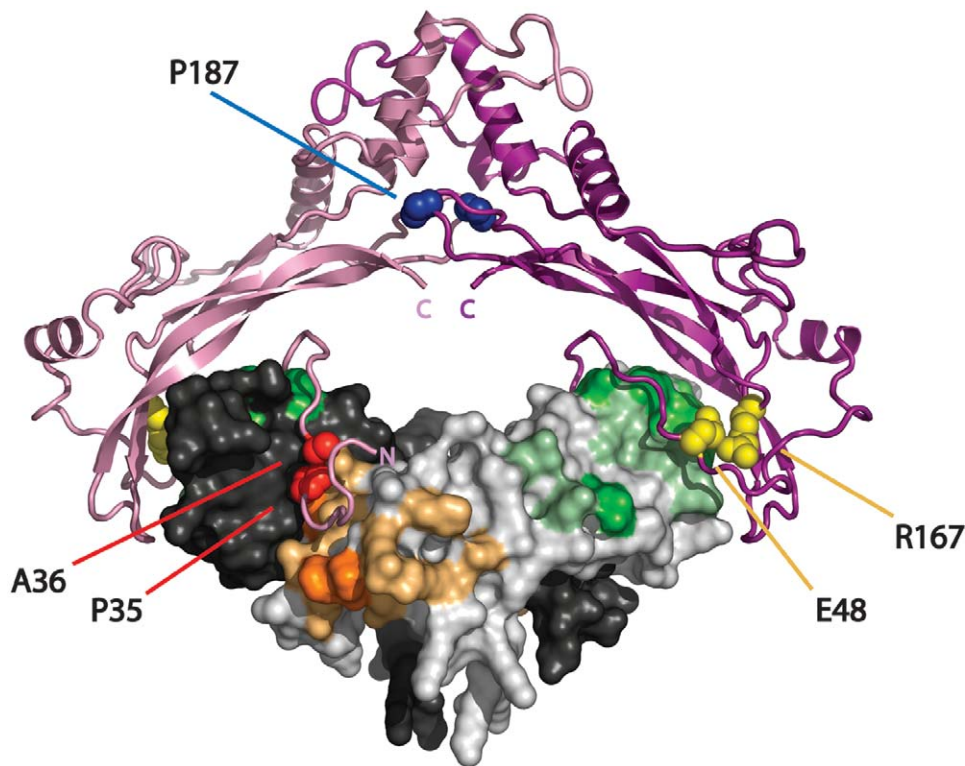


Figure 3. Three-dimensional model of NOG-GDF5 complex highlighting altered NOG amino acids found in patients with BDB2. NOG is depicted in a ribbon structure, with one monomer in dark and the second in light pink. GDF5 is shown as a surface model, with one monomer in dark and the second in light gray. Amino acids of GDF5 that interact with BMP receptor type I are highlighted in dark and light orange, and amino acids that interact with BMP receptor type II are highlighted in dark and light green. The binding of NOG to BMPs/GDFs blocks both receptor-binding sites. NOG mutations identified in patients with BDB2 are indicated. They affect three different structural clusters: (1) the site that covers the type I receptor pocket in BMPs/GDFs (P35 and A36 [red]) (2) the site that covers the type II receptor pocket (E48 and R167 [yellow]), and (3) the NOG-dimerization site (P187 [blue]).

tion. Our data indicate that a loss of NOG-GDF5 inhibition is not sufficient to explain the BDB2 phenotype.

Interestingly, the identified BDB2-associated mutations in *NOG* do not cluster on a certain domain; rather, they affect three independent regions: (1) the dimerization domain (P187, marked in blue in fig. 3), (2) the site that covers the type I receptor pocket in BMPs/GDFs (P35 and A36, marked in red in fig. 3), and (3) the site that covers the type II receptor pocket (E48 and R167, marked in yellow in fig. 3).

NOG and GDF5 are dimers linked by a disulfide bridge. The C-terminal region of NOG contains a cysteine-knot motif of nine cysteine residues that is important for disulfide-bond formation and dimerization.²⁴ One of the BDB2-causing *NOG* mutations (P187S) lies in the critical dimerization interface of NOG. This alteration destabilizes the NOG-homodimer binding, possibly influencing the overall structural integrity of the NOG-BMP complex formation. This was confirmed by western-blot analysis of supernatants of DF-1 cells expressing WT Nog or mutant variants. For the expression of Nog mutants, replication-competent avian sarcoma (RCAS) viruses containing the

coding sequence of chicken Nog (kind gift from A. Vortkamp) were digested with *Clal* and were cloned into p-SLAX-13. This construct was used for introduction of mutations into the chicken sequence of *Nog* corresponding to the human mutations P35A, P35R, P35S, A36P, R167G, and P187S, with use of the QuickChange Site-Directed Mutagenesis Kit (Stratagene) according to the manufacturer's recommendations. The coding sequence of all constructs was digested with *Clal* and was cloned into the viral vector RCASBP-B. Production and concentration of viral particles were performed as described elsewhere.³¹ Concentrated viruses of WT Nog and mutants were used to infect DF-1 cells. After cells reached confluence, the growth medium was substituted with Dulbecco's modified Eagle medium (DMEM) without fetal calf serum, and the supernatant was collected the next day. Proteins were precipitated overnight with acetone. Acetone was removed after centrifugation, and the pellet was resuspended in loading buffer for nonreducing conditions (200 mM Tris-HCl [pH 7.5], 4% SDS, 0.04% Bromophenol blue, and 40% glycerine) and reducing conditions (nonreducing buffer with 125 mM mercaptoethanol). Proteins were separated on an SDS/12%/

Table 2. Calculated Changes of Free Energy of Double Dimer Binding of NOG and GDF5

Phenotype and Mutation	dG (kcal/mol)	dG (%)	ddG (%)
Reference:			
WT Nog	-42.00	100	0
SYM1/TCC:			
P35R	-20.70	49	51
BDB2:			
P35A	-36.00	86	14
P35S	-29.00	69	31
A36P	-41.20	98	2
E48K	-41.55	99	1
R167G	-39.30	94	6
P187S	-35.10	84	16

NOTE.—Free-binding energy (dG) was calculated for binding of WT NOG or indicated NOG mutants to WT GDF5 by FOLD-X. Binding of WT NOG to WT GDF5 was set to 100% and was used as a reference for the calculated reduction of binding energy (ddG) of the NOG mutations. The SYM1/TCC (without BDB2)-associated mutation P35R resulted in the highest loss of free-binding energy (51%). In comparison, all BDB2-associated mutations showed less reduction of free-binding energy (1%–31%).

PAGE and were electroblotted onto an Immobilon-P Transfer Membrane (Millipore). Immunodetection was performed after blocking with 5% milk in PBS containing 0.2% Tween-20 with an anti-Noggin polyclonal antibody (Santa Cruz Biotechnology [catalog number sc-25656; lot number F2804]) and a secondary anti-rabbit-HRP antibody (Calbiochem [catalog number DC03L]). Signals were detected by enhanced chemiluminescence reaction (Roth) and exposure on light-sensitive films.

The P187S mutation causes a disturbance of Nog dimerization that leads to the secretion of monomeric forms. In contrast, WT Nog and the other tested Nog mutants P35R, P35S, P35A, A36P, and R167G are properly secreted as disulfide-bonded dimers (fig. 4A and 4B). We hypothesize that the mutation P187S interferes with the formation of an intermolecular disulfide bridge, thus disturbing the formation of two Nog molecules to a dimer without leading to a severe conformational change of monomeric Nog. It is possible that two mutant monomers are still able to inhibit BMPs by assembling to a dimerlike structure with antagonistic properties when binding to BMPs. This possibility is supported by the observation that overexpression of the P187S Nog mutant in the micromass culture system leads to an inhibition of endogenous chondrogenesis comparable to WT Nog (fig. 4C).

The NOG-GDF5 complex is assembled mainly by two hydrophobic areas. NOG is predicted to bind to GDFs/BMPs in a two-step mechanism. First, NOG supposedly binds the BMP receptor type II interface of BMPs, upon which the N-terminal region hinges toward the BMP receptor type I interface. Amino acids 35 and 36 are located in one of the hydrophobic regions, the so-called NOG clip domain,

spanning amino acids 28–39. This region inserts through hydrophobic interactions in the hydrophobic pocket of BMPs, thus blocking the BMP binding site for the BMP type I receptors, as depicted in figure 3. A key function at this site can be predicted for amino acid P35. With its hydrophobic ring, proline forms a direct contact to this BMP pocket.²⁴ It is highly probable that amino acid changes at this position lead to a conformational change of the N-terminal hydrophobic NOG region and therefore are likely to disturb the affinity and specificity toward certain BMPs/GDFs. An amino acid change substituting the hydrophobic proline for a polar, hydrophilic serine (P35S), as in two of the investigated families, is expected to induce a steric hindrance, because serine will not fit into the hydrophobic BMP pocket. In the case of the SYM1/TCC-associated P35R mutation, this effect can be expected to be more dramatic, possibly explaining the different phenotypic outcome.

The NOG region, amino acids 40–48, forms another hydrophobic interaction domain that is predicted to mask the interaction site of BMPs that binds to the BMP type II receptors. The mutation E48K, an amino acid change from glutamic acid to basic lysine, is likely to interfere with binding at this site. The amino acid substitution R167G, a change from hydrophobic arginine to a small uncharged glycine, is also located in a finger domain located close to this BMP receptor II site. Both mutations are likely to result in free BMP type II receptor-binding sites, possibly leading to increased binding of BMPs to their type II receptors and a shift toward the BMP type II receptor, because the BMPRI1A/B sites are still covered by NOG. The effect of this situation on BMP signaling is not entirely clear. So far, it is known that a heterodimer formation between the type I and II receptors is a necessary initial step for signal transduction in chondrogenesis. This may still be prevented by binding of mutated NOG to the type I receptor site, thus inhibiting chondrogenic differentiation, as observed in the micromass system.

Taken together, our current data show that most of the identified mutations are clustered in regions of the NOG protein that block the BMP-binding sites for the BMP receptors. This is likely to result in an enhanced or altered signaling via the BMP receptors. The importance of BMP receptors for limb development is exemplified by overexpression studies in the chick,³² gene inactivation experiments in the mouse,³³ and the identification of mutations in human limb-malformation syndromes.^{6,34,35} A disequilibrium of BMP receptor signaling caused by an altered NOG protein is likely to result in a disturbance of phalangeal development. This effect must be different from NOG loss-of-function mutations, observed in SYM1, since distal aplasia of phalanges is not observed in these patients.

For functional analyses of the BDB-associated NOG mutations, we overexpressed them by an RCAS retrovirus in the chicken limb-bud micromass culture system as described elsewhere.⁶ When cells were seeded, 1 μ l of con-

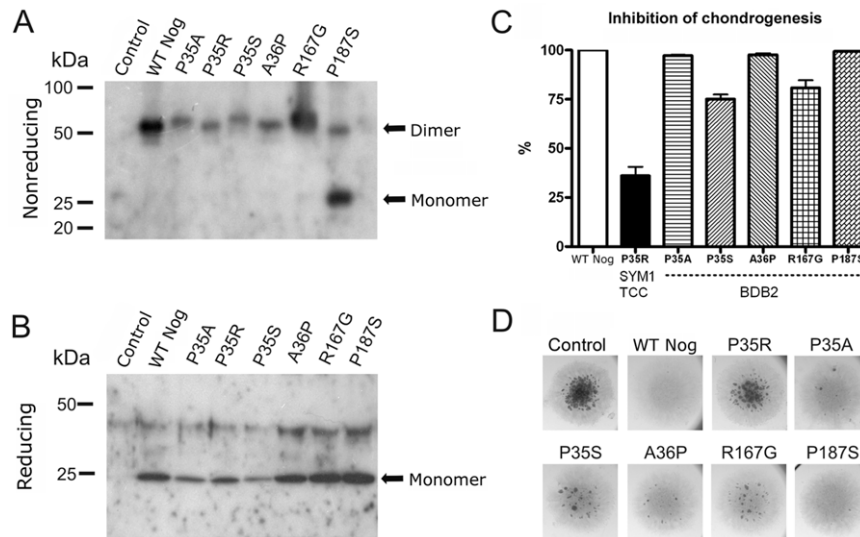


Figure 4. Secretion of Nog mutant proteins by DF-1 cells and functional analysis in the micromass culture system, with western-blot analysis of conditioned media from DF-1 cells infected with RCASBP-B containing the coding sequence of either *Nog* WT sequence (WT Nog), BDB-associated mutant sequence (P35A, P35S, A36P, R167G, and P187S), or SYM1/TCC-derived sequence (P35R). As a negative control, DF-1 cells were infected with empty RCASBP-B (control). *A*, SDS-PAGE under nonreducing conditions and immunodetection with use of anti-Nog antibody. WT Nog is secreted as a disulfide-bonded dimer, as are mutants P35A, P35R, P35S, A36P, and R167G. The mutant P187S is secreted predominantly as a monomer, and only a small amount of disulfide-bonded dimer is secreted, which supports the hypothesis that this amino acid change directly affects the dimerization of Nog. *B*, SDS-PAGE under reducing conditions and immunodetection with use of anti-Nog antibody. All Nog dimers resolve to monomers. *C*, WT Nog or indicated mutants, retrovirally overexpressed in micromass cultures from chicken limb buds and grown for 6 d in culture medium. Chondrogenic differentiation of the cultures was quantified by histomorphometric analysis of Alcian blue-stained nodules. WT Nog completely inhibited nodule formation in the micromass cultures. The inhibition of chondrogenesis by WT Nog was set to 100%. In comparison with WT Nog, the analyzed BDB2-associated Nog mutants resulted only in a minor reduction of Nog activity. P35A, A36P, and P187S showed nearly full activity, whereas P35S and R167G showed a reduction of 20%–25%. In contrast, the SYM1/TCC-associated Nog mutant P35R showed an obvious reduction of ~60% biological activity, indicating a major loss of function. *D*, Photographs of Alcian blue-stained micromass cultures.

centrated RCAS virus containing either WT *Nog* or mutant *Nog* was added per culture; uninfected cultures served as a control. For each condition, four replicates were performed in parallel. Culture medium (DMEM-F12, 10% fetal calf serum, and 0.2% chicken serum) was replaced every 2–3 d. After 6 d, micromass cultures were fixed and stained with Alcian blue. Nodule formation was quantified by histomorphometric analysis with the software tool Autmess (Zeiss) (fig. 4C and 4D). As expected, WT Nog completely prevented chondrogenic differentiation, whereas the SYM1/TCC-associated mutation P35R showed a decreased inhibitory activity resulting in an almost unaltered chondrogenic differentiation. In contrast, the BDB2-associated NOG mutants showed no major loss of biological activity in this assay. Interestingly, this also holds true for the P187S mutant, which was shown to be mainly monomeric. On the basis of these results, we conclude that the BDB2-associated mutations do not cause a simple loss of function and thus act in a different manner, probably by disturbing the intricate balance of BMP signaling in a more subtle way. Specific effects on certain BMPs or a yet-unknown interaction to other proteins are further possible explanations.

Even though the precise mechanisms of the pathogenic effect caused by the *NOG* point mutations described here are unclear, it is likely that BDB2 is a result of specific *NOG* mutations. The observed phenotype of variable BDB in combination with SYM1/TCC was a consistent feature in all of the affected individuals described here. The presence of BDB is an additional feature that distinguishes this condition from other known *NOG* joint-fusion syndromes.

The occurrence of SYM and TCC caused by mutations in the BMP-inhibitor *NOG* can possibly be explained by a partial loss of *NOG* function leading to reduced binding affinity of *NOG* to different BMPs/GDFs.²⁴ This might, among other effects, result in an increased GDF5 signaling causing abnormal joint formation. This mechanism is supported by the observation that gain-of-function mutations in GDF5 may cause SYM1 or SYNS1, most likely through the activation of *BMPR1A*, the receptor normally activated by *BMP2*.^{36,37}

Distal hypoplasia/aplasia of phalanges is associated with truncating *ROR2* mutations, but how these exert their pathogenic effect is still unknown.^{2,38,39} A direct interaction between the BMP type IB receptor (*BMPR1B*) and *ROR2* has been demonstrated elsewhere.⁴ *ROR2* and *BMPR1B* form a

ligand-independent heteromeric complex at the cell surface, leading to an activation of ROR2 through transphosphorylation by BMPR1B. An activated tyrosine kinase of ROR2 was shown to inhibit the BMPR1B pathway. It was suggested that signal transduction via both receptors is needed for proper chondrogenic differentiation. The clinical phenotype of combined BDB, SYM1, and TCC in the patients described here supports the hypothesis of a functional connection between the BMP receptors and ROR2. In addition, the observation that a *NOG* mutation at the BMP type II receptor binding site leads to distal SYM, a feature associated with *ROR2* mutations, argues for a modulating effect between the two receptors. Furthermore, patients with BDB1 can be affected by fusion of carpal bones similar to that of BDB2-affected patients with *NOG* mutations.³ The occurrence of distal SYM together with SYM1 and TCC caused by mutations at the BMP type II receptor binding site of *NOG* was observed elsewhere and confirms that distal interphalangeal joint fusion is not a coincidental feature.^{14,40} The phenotypic overlap between BDB1 and BDB2 indicates a functional connection between BMP and ROR2 signaling in vivo.

In summary, this work describes a new subtype of brachydactyly (BDB2) due to novel mutations in *NOG*. This patient group is defined by the presence of hypoplasia/aplasia of distal phalanges in combination with joint fusions. Patients with an amputation-like phenotype should have a thorough clinical and radiological evaluation of their hands and feet, to identify additional SYM and carpal or tarsal synostosis. If these joint fusions are present, a causative *NOG* mutation is very likely.

Acknowledgment

We thank the patients and family members for their participation in this study. We thank Prof. Coskun Silan for his support in collecting clinical data. We acknowledge the technical help of Gundula Leschik, Randi Koll, Elena Bochukova, and Mike Oldridge. This work was partially funded by Deutsche Forschungsgemeinschaft grant LE 1851/1-1 (to K.L.), Sonderforschungsbereich grant 760 (to P.S. and S. Mundlos), the Birth Defects Foundation (support to A.O.M.W.), and the Wellcome Trust (support to A.O.M.W.). The Wilhelm Johannsen Center was established by the National Danish Research Foundation. K.W.K was supported by the Ib Mogens Kristiansen Almene Fond.

Web Resources

Accession numbers and URLs for data presented herein are as follows:

GenBank, <http://www.ncbi.nlm.nih.gov/Genbank/> (for *ROR2* [accession number NM_004560] and *NOG* [accession number NM_005450])

Online Mendelian Inheritance in Man (OMIM), <http://www.ncbi.nlm.nih.gov/Omim/> (for BDB1, SYM1, TCC, SYNS1, and stapes ankylosis with broad thumb and toes without SYM)

PDB, <http://www.rcsb.org/pdb/home/home.do>

References

- Bell J (1951) On brachydactyly and symphalangism. In: Penrose, LS (ed) Treasury of human inheritance. Vol 5. Cambridge University Press, London, United Kingdom, pp 1–31
- Oldridge M, Fortuna AM, Maringa M, Propping P, Mansour S, Pollitt C, DeChiara TM, Kimble RB, Valenzuela DM, Yancopoulos GD, et al (2000) Dominant mutations in *ROR2*, encoding an orphan receptor tyrosine kinase, cause brachydactyly type B. *Nat Genet* 24:275–278
- Schwabe GC, Tinschert S, Buschow C, Meinecke P, Wolff G, Gillissen-Kaesbach G, Oldridge M, Wilkie AOM, Komec R, Mundlos S (2000) Distinct mutations in the receptor tyrosine kinase gene *ROR2* cause brachydactyly type B. *Am J Hum Genet* 67:822–831
- Sammar M, Stricker S, Schwabe GC, Sieber C, Hartung A, Hanke M, Oishi I, Pohl J, Minami Y, Sebald W, et al (2004) Modulation of GDF5/BRI-b signalling through interaction with the tyrosine kinase receptor *Ror2*. *Genes Cells* 9:1227–1238
- Schwabe GC, Turkmen S, Leschik G, Palanduz S, Stover B, Goecke TO, Mundlos S (2004) Brachydactyly type C caused by a homozygous missense mutation in the prodomain of CDMP1. *Am J Med Genet A* 124:356–363
- Lehmann K, Seemann P, Stricker S, Sammar M, Meyer B, Surin K, Majewski F, Tinschert S, Grzeschik KH, Muller D, et al (2003) Mutations in *bone morphogenetic protein receptor 1B* cause brachydactyly type A2. *Proc Natl Acad Sci USA* 100:12277–12282
- Gong Y, Krakow D, Marcelino J, Wilkin D, Chitayat D, Babul-Hirji R, Hudgins L, Cremers CW, Cremers FP, Brunner HG, et al (1999) Heterozygous mutations in the gene encoding *noggin* affect human joint morphogenesis. *Nat Genet* 21:302–304
- Dixon ME, Armstrong P, Stevens DB, Bamshad M (2001) Identical mutations in *NOG* can cause either tarsal/carpal coalition syndrome or proximal symphalangism. *Genet Med* 3: 349–353
- Marcelino J, Sciortino CM, Romero MF, Ulatowski LM, Balllock RT, Economides AN, Eimon PM, Harland RM, Warman ML (2001) Human disease-causing *NOG* missense mutations: effects on *noggin* secretion, dimer formation, and bone morphogenetic protein binding. *Proc Natl Acad Sci USA* 98: 11353–11358
- Brown DJ, Kim TB, Petty EM, Downs CA, Martin DM, Strouse PJ, Moroi SE, Milunsky JM, Lesperance MM (2002) Autosomal dominant stapes ankylosis with broad thumbs and toes, hyperopia, and skeletal anomalies is caused by heterozygous nonsense and frameshift mutations in *NOG*, the gene encoding *noggin*. *Am J Hum Genet* 71:618–624
- Herrmann J (1974) Symphalangism and brachydactyly syndrome: report of the WL symphalangism-brachydactyly syndrome. *Birth Defects Orig Artic Ser* 10:23–53
- Maroteaux P, Bouvet JP, Briard ML (1972) [Multiple synostosis disease.] *Nouv Presse Med* 1:3041–3047
- Oldridge M, Temple IK, Santos HG, Gibbons RJ, Mustafa Z, Chapman KE, Loughlin J, Wilkie AOM (1999) Brachydactyly type B: linkage to chromosome 9q22 and evidence for genetic heterogeneity. *Am J Hum Genet* 64:578–585
- Kosaki K, Sato S, Hasegawa T, Matsuo N, Suzuki T, Ogata T (2004) Premature ovarian failure in a female with proximal symphalangism and *Noggin* mutation. *Fertil Steril* 81:1137–1139

15. Mangino M, Flex E, Digilio MC, Giannotti A, Dallapiccola B (2002) Identification of a novel NOG gene mutation (P35S) in an Italian family with symphalangism. *Hum Mutat* 19:308
16. Brunet LJ, McMahon JA, McMahon AP, Harland RM (1998) Noggin, cartilage morphogenesis, and joint formation in the mammalian skeleton. *Science* 280:1455–1457
17. Francis-West PH, Abdelfattah A, Chen P, Allen C, Parish J, Ladher R, Allen S, MacPherson S, Luyten FP, Archer CW (1999) Mechanisms of GDF-5 action during skeletal development. *Development* 126:1305–1315
18. Storm EE, Kingsley DM (1999) GDF5 coordinates bone and joint formation during digit development. *Dev Biol* 209:11–27
19. Francis-West PH, Parish J, Lee K, Archer CW (1999) BMP/GDF-signalling interactions during synovial joint development. *Cell Tissue Res* 296:111–119
20. Nifuji A, Noda M (1999) Coordinated expression of noggin and bone morphogenetic proteins (BMPs) during early skeletogenesis and induction of noggin expression by BMP-7. *J Bone Miner Res* 14:2057–2066
21. Gilboa L, Nohe A, Geissendorfer T, Sebald W, Henis YI, Knaus P (2000) Bone morphogenetic protein receptor complexes on the surface of live cells: a new oligomerization mode for serine/threonine kinase receptors. *Mol Biol Cell* 11:1023–1035
22. Nohe A, Keating E, Knaus P, Petersen NO (2004) Signal transduction of bone morphogenetic protein receptors. *Cell Signal* 16:291–299
23. Balemans W, Van Hul W (2002) Extracellular regulation of BMP signaling in vertebrates: a cocktail of modulators. *Dev Biol* 250:231–250
24. Groppe J, Greenwald J, Wiater E, Rodriguez-Leon J, Economides AN, Kwiatkowski W, Affolter M, Vale WW, Belmonte JC, Choe S (2002) Structural basis of BMP signalling inhibition by the cystine knot protein Noggin. *Nature* 420:636–642
25. Nishitoh H, Ichijo H, Kimura M, Matsumoto T, Makishima F, Yamaguchi A, Yamashita H, Enomoto S, Miyazono K (1996) Identification of type I and type II serine/threonine kinase receptors for growth/differentiation factor-5. *J Biol Chem* 271:21345–21352
26. Kirsch T, Nickel J, Sebald W (2000) BMP-2 antagonists emerge from alterations in the low-affinity binding epitope for receptor BMPR-II. *EMBO J* 19:3314–3324
27. Massague J, Chen Y-G (2000) Controlling TGF- β signaling. *Genes Dev* 14:627–644
28. Schreuder H, Liesum A, Pohl J, Kruse M, Koyama M (2005) Crystal structure of recombinant human growth and differentiation factor 5: evidence for interaction of the type I and type II receptor-binding sites. *Biochem Biophys Res Commun* 329:1076–1086
29. Gao Y, Lai L (2004) Structure-based method for analyzing protein-protein interfaces. *J Mol Model* 10:44–54
30. Guerois R, Nielsen JE, Serrano L (2002) Predicting changes in the stability of proteins and protein complexes: a study of more than 1000 mutations. *J Mol Biol* 320:369–387
31. Morgan BA, Fekete DM (1996) Manipulating gene expression with replication-competent retroviruses. *Methods Cell Biol* 51:185–218
32. Zou H, Wieser R, Massague J, Niswander L (1997) Distinct roles of type I bone morphogenetic protein receptors in the formation and differentiation of cartilage. *Genes Dev* 11:2191–2203
33. Yoon BS, Ovchinnikov DA, Yoshii I, Mishina Y, Behringer RR, Lyons KM (2005) *Bmpr1a* and *Bmpr1b* have overlapping functions and are essential for chondrogenesis in vivo. *Proc Natl Acad Sci USA* 102:5062–5067
34. Demirhan O, Turkmen S, Schwabe GC, Soyupak S, Akgul E, Tastemir D, Karahan D, Mundlos S, Lehmann K (2005) A homozygous *BMPR1B* mutation causes a new subtype of acromesomelic chondrodysplasia with genital anomalies. *J Med Genet* 42:314–317
35. Lehmann K, Seemann P, Boergermann J, Morin G, Reif S, Knaus P, Mundlos S (2006) A novel R486Q mutation in *BMPR1B* resulting in either a brachydactyly type C/symphalangism-like phenotype or brachydactyly type A2. *Eur J Hum Genet* 14:1248–1254
36. Seemann P, Schwappacher R, Kjaer KW, Krakow D, Lehmann K, Dawson K, Stricker S, Pohl J, Ploger F, Staub E, et al (2005) Activating and deactivating mutations in the receptor interaction site of GDF5 cause symphalangism or brachydactyly type A2. *J Clin Invest* 115:2373–2381
37. Dawson K, Seeman P, Sebald E, King L, Edwards M, Williams J III, Mundlos S, Krakow D (2006) *GDF5* is a second locus for multiple-synostosis syndrome. *Am J Hum Genet* 78:708–712
38. Afzal AR, Jeffery S (2003) One gene, two phenotypes: ROR2 mutations in autosomal recessive Robinow syndrome and autosomal dominant brachydactyly type B. *Hum Mutat* 22:1–11
39. Stricker S, Verhey van Wijk N, Witte F, Brieske N, Seidel K, Mundlos S (2006) Cloning and expression pattern of chicken *Ror2* and functional characterization of truncating mutations in brachydactyly type B and Robinow syndrome. *Dev Dyn* 235:3456–3465
40. Debeer P, Huysmans C, Van de Ven WJ, Fryns JP, Devriendt K (2005) Carpals and tarsals synostoses and transverse reduction defects of the toes in two brothers heterozygous for a double de novo NOGGIN mutation. *Am J Med Genet A* 134:318–320